Available online at www.sciencedirect.com
ScienceDirect
Journal of Power Sources 171 (2007) 506–510
JOURNAL OF POWER SOURCES
www.elsevier.com/locate/jpowsour

Short communication

Ionic conductivity of Sm, Gd, Dy and Er-doped ceria

Sutin Kuharuangrong *

School of Ceramic Engineering, Suranaree University of Technology, Nakhon Ratchasima 30000, Thailand

Received 11 March 2007; received in revised form 15 May 2007; accepted 22 May 2007
Available online 19 June 2007

Abstract

Ceria-based materials are prospective electrolytes for intermediate-temperature solid oxide fuel cells. The ionic conductivities of ceria-doped with Sm, Gd, Dy and Er are investigated as a function of temperature by using a.c. impedance. The results show that conductivity depends on the rare earth dopant, its amount, an appearance of second phase, and the microstructure. With 10 mol% dopant, Sm exhibits higher conductivity than Gd, Dy and Er, respectively. With an increase in Dy content, the total conductivity increases, which is attributed to an increase in grain boundary conductivity. By contrast, an increasing amount of Er from 10 to 20 mol% reduces the conductivity of ceria and results in a separated phase of Er_2O_3 as detected by X-ray diffraction and scanning electron microscopy. In addition, the grain size corresponding to grain boundary density affects the conductivity due to the contributions from the grain interior and grain boundary conductivities.

Keywords: Ceria; Intermediate-temperature; Solid oxide fuel cell; Ionic conductivity; Electrical conductivity; Electrolyte; Rare earth dopants

1. Introduction

Ceria-based materials have been extensively studied as the most promising electrolytes for intermediate-temperature solid oxide fuel cell (SOFC). Their ionic conductivities at 750 °C are similar to that of Yttria-stablized zirconia (YSZ) at 1000 °C [1], although they are not pure ionic conductors. A transition from ionic to electronic conductivity depends on the grain size due to the space charge potential along the grain boundaries [2]. It also depends on the partial pressure of O_2 for the Ce^{4+} to Ce^{3+} transformation [3,4]. The ionic conductivity of ceria resulting from oxygen vacancies depends on the dopants and their amount [5–8]. It increases significantly when ceria is doped with aliovalent oxides such as Y_2O_3 and various rare earth oxides. However, an increasing amount of dopants tends to form a second phase due to the solubility limit, and this reduces the conductivity. The critical dopant concentration to achieve the total conductivity was reported to be approximately 20 mol%, which was due to the formation of microdomains [9]. Balazs and Glass [10] reported that the addition of 10 mol% dopants did not appear to affect the sintering properties with the exception of some rare earths. They also reported that the ionic radius of the dopant did not affect the conductivity of ceria. From their results, Gd, Sm and Y exhibited higher conductivity than Nd, Dy and Er. On the other hand, Eguchi et al. work [11] found that Sm, Gd and Dy gave high ionic conductivity. Steele [4] reported that the ionic conductivity at 500 °C of $Ce_{0.9}Gd_{0.1}O_{1.95}$ was higher than that of $Ce_{0.887}Y_{0.113}O_{1.9435}$, $Ce_{0.8}Gd_{0.2}O_{1.9}$ and $Ce_{0.9}Sm_{0.1}O_{1.95}$, respectively.

In this work, Sm, Gd, Dy and Er are selected as dopants of ceria due to their lower charge and similar cation size. The effects of these dopants and their amount on the electrical conductivity and microstructure of ceria are investigated and compared. In addition, the contributions from grain interior and grain boundary conductivities to the total conductivity of doped ceria are presented.

2. Experimental procedure

All doped-ceria compositions were prepared by a solid-state reaction method from oxide materials (99.9% purity). The powders were mixed by ball-milling with zirconia balls and absolute ethanol. After drying and calcining at 1200 °C, the phase of each composition was determined by X-ray diffraction (XRD, Jeol JDX3530) phase analysis. The calcined powder was pressed into pellets with a uniaxial hydraulic press, followed by a

* Tel.: +66 44 224474; fax: +66 44 224462.
E-mail address: sutin@sut.ac.th.

0378-7753/$ – see front matter © 2007 Elsevier B.V. All rights reserved.
doi:10.1016/j.jpowsour.2007.05.104

cold-isostatic press at 250 MPa. All doped-ceria materials were sintered at 1500 °C with a soaking time of 5 h.

The a.c. impedance data of sintered pellets were collected with a Solartron 1260 instrument as a function of frequency and run through a Zview program. A fired-on gold electrode was applied on both sides before measurement. All impedance data were collected in air and sample temperatures were recorded with a thermocouple type K mounted close to the sample. It was assumed that the electronic contribution to the overall conductivity was minimal since all measurements were performed in air at a temperature less that 700 °C. In addition, the transport number of the oxide ion in 20 mol% Gd- or Sm-doped ceria was reported to be 0.83–0.85 at 700 °C under an oxygen partial pressure of 10^{-15} Pa [12]. Furthermore, the ionic conductivity of ceria increased greatly with decrease in temperature.

The microstructure of the specimens was observed by means of a scanning electron microscope (SEM, Jeol JSM5410). The samples were polished and thermally etched before gold sputtering.

3. Results and discussion

3.1. Phase composition

The XRD patterns of calcined powder of cation-doped ceria are shown in Fig. 1. The data show that 10 mol% Sm-, 10 mol% Er-, 20 and 30 mol% Dy-, 20 and 30 mol% Gd-doped ceria exhibit the same phase and structure. Only that of 20 mol% Er-doped ceria reveals the additional small peaks of Er_2O_3 (JCPDS no. 08-0050) raw material as indicated by arrows in the pattern. This implies that 20 mol% of Er dopant is beyond the solubility limit of ceria.

3.2. Electrical conductivity

Fig. 2 presents the impedance spectra of 10, 20 and 30 mol% Dy-doped ceria measured in air at 600 °C. These spectra are generally associated with the resistances of crystal lattice, grain boundary and electrode, which can be observed from the first, second and third arcs. Those arcs can be seen at lower frequencies at low temperatures. At high temperatures, the time constants decrease and the arcs shift to higher frequencies. Therefore, only parts of the arcs appear in the limited frequency range of equipment. The crystal lattice and grain boundary arcs are associated with the capacitances in the pF and nF ranges, respectively, determined from $2\pi f_{max}RC = 1$, where f_{max} is the applied frequency at arc maximum and R is the arc magnitude. The two arcs for all Dy-doped ceria samples observed in Fig. 2 respond to the contributions from grain boundary and electrode at 600 °C. The results show that the grain boundary resistivity of ceria observed from the magnitude of the first arc significantly decreases with an increase in Dy content while the lattice resistivity obtained from the left intercept of the first arc increases gradually. Therefore, the total conductivity from grain and grain boundary increases with the amount of Dy. The activation energies of these compositions calculated from the slope of Arrhenius plot of total conductivity are in the range of 1.06–1.15 eV, as listed in Table 1. It should be noted that the electrode resistance is neglected and will not be investigated in this work.

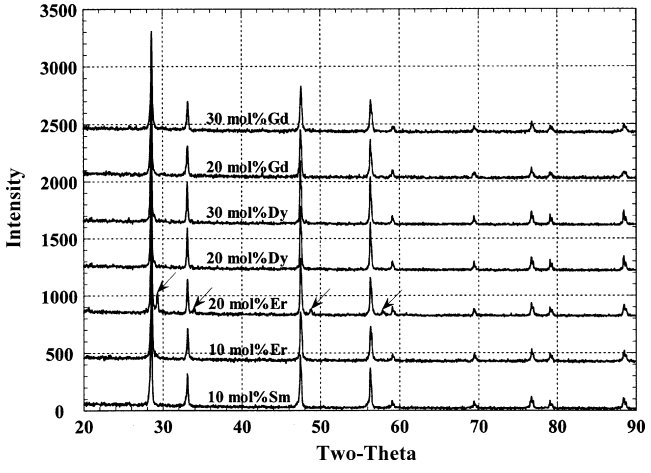

Fig. 1. XRD patterns of ceria doped with rare earths.

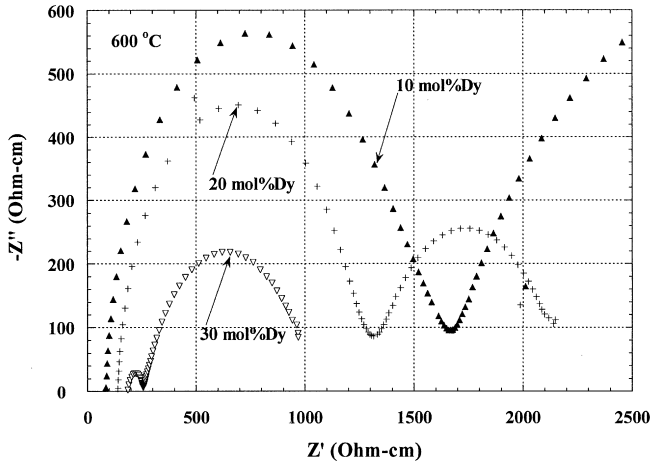

Fig. 2. Complex impedance spectra of 10, 20 and 30 mol% Dy-doped ceria at 600 °C.

The effect of Er on the resistivity of ceria at 500 °C is shown on Fig. 3. An increasing amount of Er from 10 to 20 mol% increases the resistivity of ceria. This is possibly due to the erbium oxide phase, which can be detected from XRD as shown in Fig. 1, contributing to the higher resistivity. The activation energy for both of 10 and 20 mol% Er-doped ceria is 1.15 eV.

Fig. 4 shows the temperature dependence of the total conductivity (σ_T) for Sm, Gd, Dy and Er-doped into ceria. For a doped

Table 1
Activation energies (E_A) for doped-ceria

Dopant	Amount (mol%)	E_A (eV)
Sm	10	1.00
Gd	10	1.03
Dy	10	1.06
	20	1.11
	30	1.15
Er	10	1.15
	20	1.15

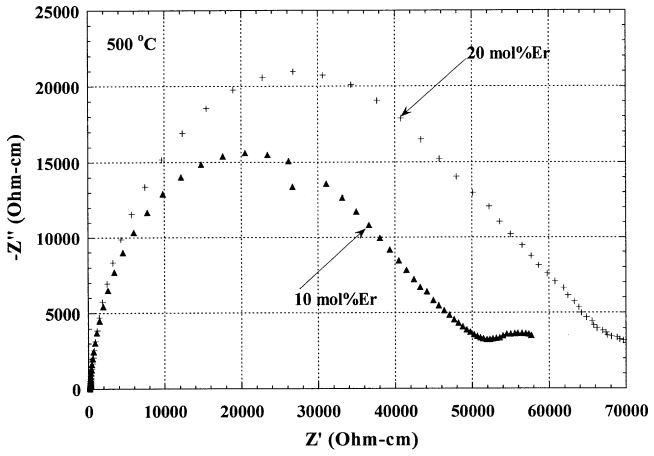

Fig. 3. Complex impedance spectra of 10 and 20 mol% Er-doped ceria at 500 °C.

amount of 10 mol%, Sm exhibits higher conductivity than Gd, Dy and Er, respectively. This result is in agreement with the previous work [10,11]. Furthermore, the observed result for ionic conductivity of 30 mol% Dy is higher than that of 10 mol% Sm. This indicates that an increase in Dy content enhances the total conductivity of ceria. The activation energies for all these compositions calculated from the slope of these plots are listed in Table 1.

Fig. 5 shows the Arrhenius plots of grain conductivity σ_g, grain boundary conductivity σ_{gb} and the total conductivity σ_T for 10 mol% Sm-doped ceria. At high temperatures, both the grain and grain boundary data show a curvature in opposite directions. At low temperature, the activation energy for the grain conductivity depends on the migration enthalpy of oxygen ions and the association enthalpy of rare earth dopants with oxygen vacancies [Re'_{Ce}-$V_O \cdot \cdot$] defect complexes [13]. At high temperatures, only migration of oxygen ions is taking place and all oxygen vacancies are free. These free vacancies are possibly trapped at the grain boundaries and this results in limited available vacancies and therefore an increase in the activation energy of grain boundary conductivity. The value of the association enthalpy depends on the interaction of rare earth dopants with oxygen

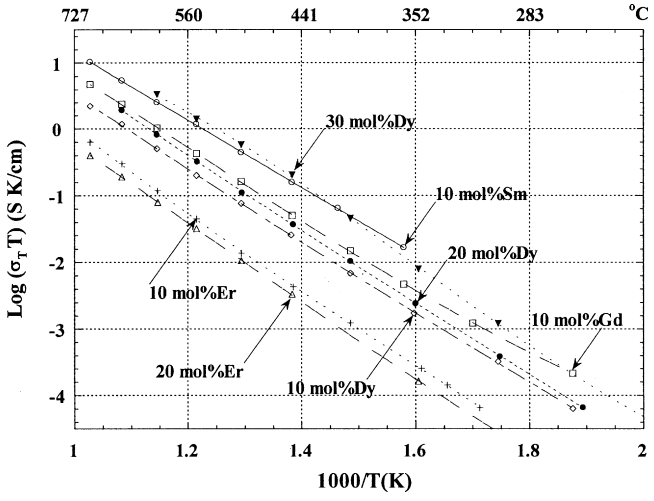

Fig. 4. Temperature dependence of total conductivity of doped ceria.

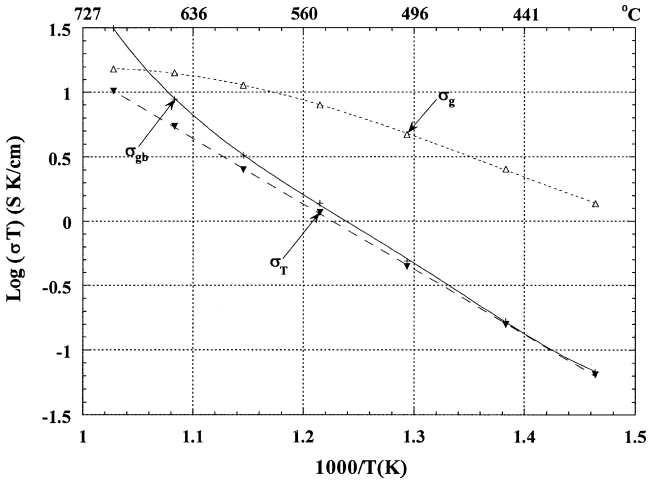

Fig. 5. Temperature dependence of grain conductivity σ_g, grain boundary conductivity σ_{gb} and total conductivity σ_T of 10 mol% Sm-doped ceria.

vacancies. In this work, Sm shows significant effect compared with Gd, Dy and Er.

Fig. 6 shows the temperature dependence of σ_g, σ_{gb} and σ_T of 10 and 30 mol% Dy-doped ceria. The results show that the σ_{gb} of 10 mol% Dy-doped ceria is much lower than the σ_g. It has been found in other works [14,15] that the presence of SiO_2 introduced from the raw materials or impurities from sample preparation can dramatically reduce the σ_{gb} of ceria and zirconia. However, for high purity materials in which silica was not detected by transmission electron microscopy the, σ_g has been reported to be higher than the σ_{gb} [16]. From this investigation, the results show that the σ_g of 10 mol% Dy-doped ceria is much higher than the σ_{gb} and σ_T. In general, both of the grain interior and grain boundary contribute to the total conductivity. For 10 mol% Dy-doped ceria, the contribution from the grain boundary to the total conductivity dominates so that the overall conductivity is approximately equal to the σ_{gb}. Obviously, σ_{gb} of ceria can increase with an increase in Dy content and the σ_{gb} is higher than the σ_g for 30 mol% Dy-doped ceria. In this

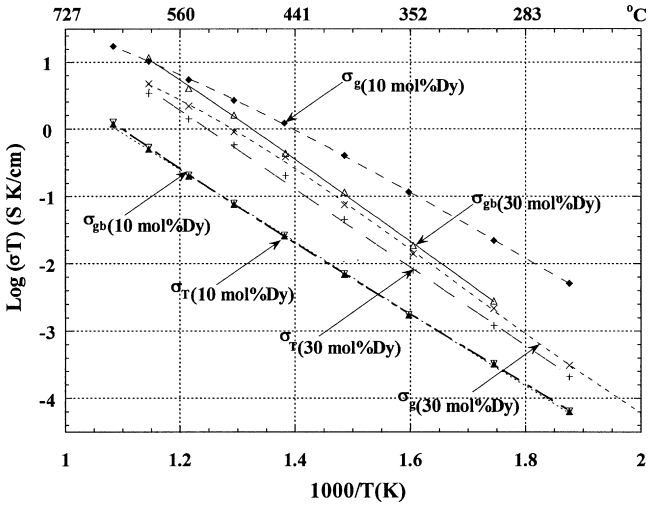

Fig. 6. Temperature dependence of grain conductivity σ_g, grain boundary conductivity σ_{gb} and total conductivity σ_T of 10 and 30 mol% Dy-doped ceria.

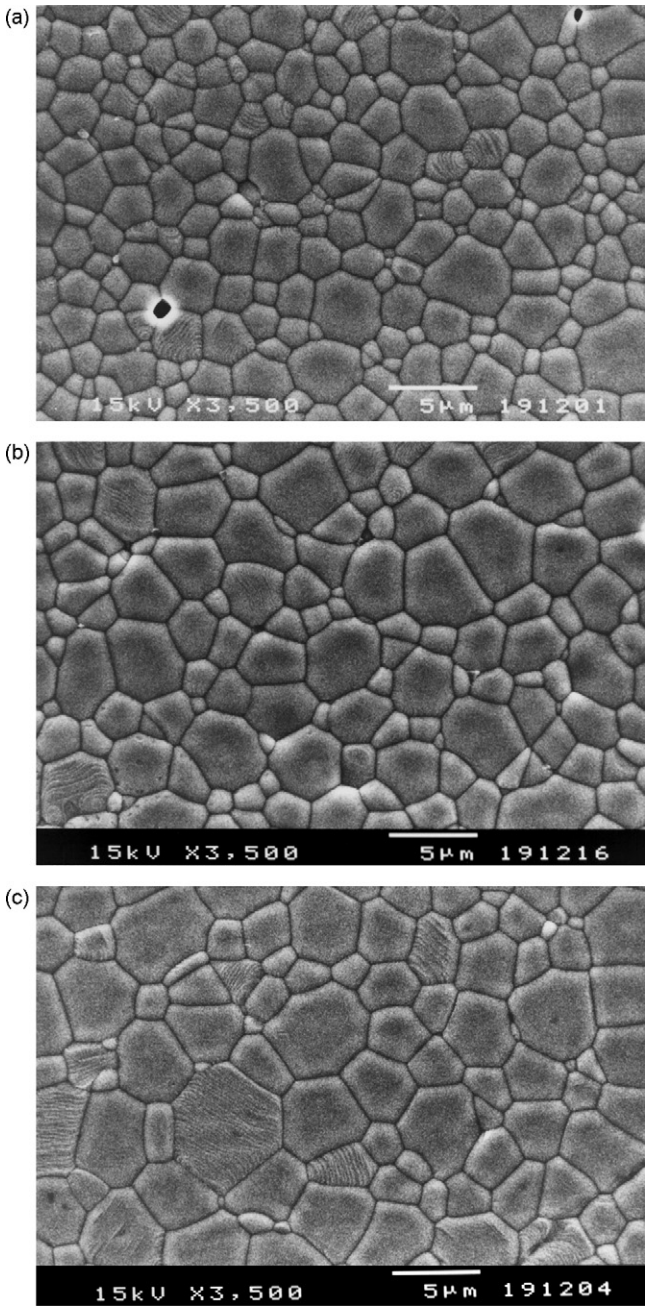

Fig. 7. Scanning electron micrographs of polished, thermally etched cross-section surface of: (a) 10 mol% Dy-doped ceria; (b) 20 mol% Dy-doped ceria; (c) 30 mol% Dy-doped ceria.

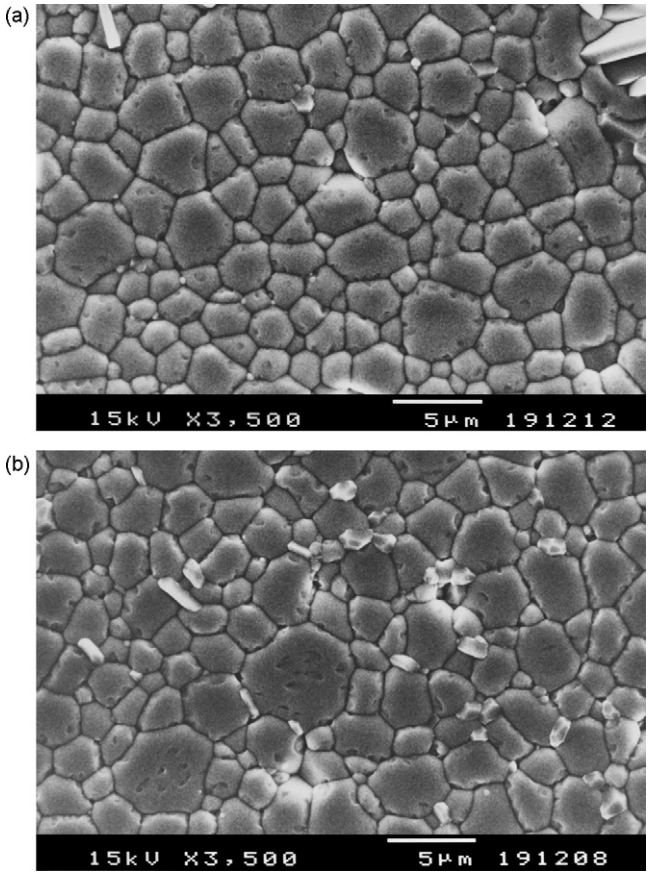

Fig. 8. Scanning electron micrographs of polished, thermally etched cross-section surfaces of: (a) 10 mol% Er-doped ceria and (b) 20 mol% Er-doped ceria.

experimental study, the σ_T is close to the σ_g, which is due to the domination from the contribution of the grain.

3.3. Microstructure

Scanning electron micrographs of Dy-doped ceria sintered at 1500 °C are illustrated in Fig. 7a–c. Apparently, an increasing amount of Dy can increase the grain size of ceria. This effect is possibly related to the conductivity results in Fig. 6, in which smaller grain sizes corresponding to large areas of grain boundary influence the σ_T of 10 mol% Dy-doped ceria, while larger grains corresponding to the contribution of grain conductivity affect the σ_T of 30 mol% Dy-doped ceria. This suggests that the higher conductivity of 30 mol% Dy-doped ceria should be obtained from the smaller grains. Therefore, if the desired microstructure can be performed, the maximum value of ionic conductivity can be achieved. Fig. 8a-b shows the photomicrographs of Er-doped ceria. A second phase can be observed in the micrograph of 20 mol% Er-doped ceria, which is consistent with the XRD result in Fig. 1 in which the small peaks of Er_2O_3 appear in this composition. This second phase possibly reduces the ionic conductivity of ceria compared with that of 10 mol% Er-doped ceria.

4. Conclusions

Sm-doped ceria exhibits the highest conductivity with respect to Gd-, Dy- and Er-doped ceria at the same doping level. The σ_T tends to increase with increasing amount of dopants. However, an increase in Er content reduces the σ_T due to the solubility limit being exceeded and Er_2O_3 is separated from the solid solution, as detected by XRD and SEM. In addition, the maximum value of ionic conductivity for each dopant can be achieved by controlling the microstructure since both of the grain interior and grain boundary contribute to the total conductivity.

Acknowledgement

This work was supported from the National Metal and Materials Technology Center.

References

[1] T. Kudo, H. Obayashi, J. Electrochem. Soc. 122 (1975) 142–147.
[2] A. Tschope, Solid State Ionics 139 (2001) 267–280.
[3] H.L. Tuller, A.S. Nowick, J. Electrochem. Soc. 122 (1975) 255–259.
[4] B.C.H. Steele, Solid State Ionics 129 (2000) 95–110.
[5] H. Yahiro, K. Eguchi, H. Arai, Solid State Ionics 36 (1989) 71–75.
[6] G.B. Balazs, R.S. Glass, Proceedings of 2nd International Symposium on Ionic and Mixed Conducting Ceramics, Electrochemical Society, 1994, p. 478.
[7] H. Inaba, H. Tagawa, Solid State Ionics 83 (1996) 1–16.
[8] M. Mogensen, N.M. Sammes, G.A. Tompsett, Solid State Ionics 129 (2000) 63–94.
[9] T.S. Zhang, J. Ma, L.B. Kong, S.H. Chan, J.A. Kilner, Solid State Ionics 170 (2004) 209–217.
[10] G.B. Balazs, R.S. Glass, Solid State Ionics 76 (1995) 155–162.
[11] K. Eguchi, T. Setoguchi, T. Inoue, H. Arai, Solid State Ionics 52 (1992) 165–172.
[12] T. Shimonosono, Y. Hirata, Y. Ehira, S. Sameshima, T. Horita, J. Ceram Soc. Jpn. Suppl. 112 (2004) S264.
[13] J.A. Kilner, B.C.H. Steele, in: O.T. Sorensen (Ed.), Nonstoichiometric Oxides, Academic Press, New York, 1981, p. 233.
[14] D.Y. Wang, A.S. Nowick, J. Solid State Chem. 35 (1980) 325–333.
[15] R. Gerhardt, A.S. Nowick, J. Am. Ceram. Soc. 69 (1986) 641–646.
[16] M. Aoki, Y.M. Chiang, I. Kosacki, J.R. Lee, H. Tuller, Y. Liu, J. Am. Ceram. Soc. 79 (1996) 1169–1180.